applied sciences

MDPI

Article

Assessing the Impact of Sensor Orientation on Accelerometer-Derived Angles: A Systematic Analysis and Proposed Error Reduction

Frederick A. McClintock, Andrew J. Callaway, Carol J. Clark and Jonathan M. Williams *

Faculty of Health and Social Sciences, Bournemouth University, Fern Barrow, Poole BH12 5BB, UK; fmcclintock@bournemouth.ac.uk (F.A.M.); acallaway@bournemouth.ac.uk (A.J.C.); cclark@bournemouth.ac.uk (C.J.C.)

* Correspondence: jwilliams@bournemouth.ac.uk

Abstract: Accelerometers have been widely used for motion analysis. The effect of initial sensor orientation (ISO) on the derived range of motion (ROM) is currently unexplored, limiting clarity in understanding error. This two-step study systematically explored the effect of ISO on the error of accelerometer-derived range of motion (ROM) and the effect of a proposed correction algorithm. Accelerometer data were used to compute peak and through-range ROM across a range of ISO and movement angular velocities up to 148° s^{-1} compared to an optoelectronic gold-standard. Step 1 demonstrated that error increased linearly with increasing ISO offsets and angular velocity. Average peak ROM RMSE at an ISO of 20° tilt and twist was 5.9° for sagittal motion, and for an ISO of 50° pitch and 20° twist, it was 7.5° for frontal plane ROM. Through-range RMSE demonstrated errors of 7–8° for similar ISOs. Predictive modeling estimated a 3.2° and 3.7° increase in peak and through-range sagittal plane error for every 10° increase in tilt and twist ISO. Step 2 demonstrated error reduction utilizing mathematical correction for ISO, resulting in <1° mean peak error and <1.2° mean through-range ROM error regardless of ISO. Accelerometers can be used to measure cardinal plane joint angles, but initial orientation is a source of error unless corrected.

Keywords: accelerometers; human motion; joint angle; motion analysis; sensors

Citation: McClintock, F.A.; Callaway, A.J.; Clark, C.J.; Williams, J.M. Assessing the Impact of Sensor Orientation on Accelerometer-Derived Angles: A Systematic Analysis and Proposed Error Reduction. *Appl. Sci.* **2024**, *14*, 842. https://doi.org/10.3390/app14020842

Academic Editor: Fausto Famà

Received: 19 December 2023
Revised: 5 January 2024
Accepted: 16 January 2024
Published: 19 January 2024

1. Introduction

Human movement analysis has traditionally been the domain of the laboratory, where optoelectronic systems have been the gold standard [1,2]. Their use remains the cornerstone of practice in biomechanics and kinesiology. However, they remain expensive and require a designated environment. This limits their use in the routine assessment of movement, real-world testing of movement behavior, or studying movement behavior across long time periods. Improving accessibility to these measurements is crucial for the future of the industry.

One solution to the above limitations would be to employ body-worn sensors. Sensors such as accelerometers [3], gyroscopes [4], and full inertial measurement units (IMUs) [5] have all been used to quantify movement. These systems have been shown to be reliable [4,6–8] and valid [9–13] compared to an optoelectronic gold standard. Established validity and reliability of these sensor systems against optoelectronic gold standards have focused on the difference between measured peak angles [7,9,14]. This method of assessment lacks nuance and ecological validity compared to the anticipated use on humans, where data are likely to be evaluated over a range of movement, such as through movement behavior across time, and not just static peak values.

In isolation, gyroscopes rely on integration from angular velocity to produce angular displacement, and this is prone to drift over time due to the integration of noise and non-zero gyroscope bias [15], making these of limited use for prolonged data collection sessions.

IMUs, with their integrated technology and fusion algorithms, often use magnetometers to overcome challenges with sensor drift by providing an absolute heading reference [16]. However, the magnetic field vector is disturbed by metals and electronic devices, meaning that data collection in real-world environments is difficult [17].

Accelerometers, if used in isolation, provide estimates of linear acceleration but can be used to compute angles through the known relationship with the gravity vector [18]. The computation is relatively simple as it does not rely on complex fusion algorithms, and accelerometers do not have problems with drift or metallic interference, making them an attractive option for wearable sensors. However, the orientation of the accelerometer sensor is computed relative to the vertical gravity vector. Therefore, if the sensor is rotated about the vertical gravity vector, no change in orientation is determined, thus restricting the angles to only two planes of motion [19]. Furthermore, accuracy of the gravity vector is reliant on the sensors being relatively still, as any motion results in acceleration in addition to the acceleration of gravity. This results in the sensor output being a combination of accelerations, affecting further mathematical calculations. Whilst accelerometers have been applied to spinal movement analysis [10,20], some important sources of error have not been systematically assessed, which could affect their accuracy for clinical use.

Wearable sensors for human movement analysis are prone to many sources of error including, but not limited to, the sensor itself, human variability, and the interface between the sensor and human. This human–sensor interaction as a source of error is the error associated with the interface between the physical device (sensor) and the human, i.e., the attachment. Previous research has focused on errors associated with soft tissue artifacts, where there is movement of the soft tissues over the underlying bones [21,22]. Whilst this is an important consideration, it exists for all surface methods of measuring motion. Other sources of human–sensor interaction error may include issues with the fixation such that the fixation fails non-uniformly, resulting in sensor movement which is not mapping body movement. However, error may also relate to the initial orientation of the sensor.

Consistent alignment of the sensors axes to the human body is virtually impossible. It is not ideal for clinicians or coaches to be burdened with trying to attach devices in a specific orientation with a high level of precision. This is also demonstrated where different operators are present (i.e., inter-operator error), as well as errors associated with removing and reattaching measurement devices (i.e., pre–post intervention/follow-up data collection attachment error). Therefore, the effects of different sensor attachment orientations on error amount to an important consideration. This is particularly important for 'before and after' comparisons, where confidence is needed in any observed change representing a true change of the human and not just an attachment error.

To date, many studies have employed accelerometers to measure angles [20,23,24]. Despite this common use of accelerometers, it is not clear if initial sensor orientation angle has been considered in the quantification of the angles or ROM reported. For example, previously reported limits of agreement between gold standard methods and accelerometers, without correcting for initial orientation, range from –8.06° to 5.67° [25] and −3.86° to 4.69° [11], meaning that 95% of future paired observations are likely to fall between this range of error. These error ranges are large, and it is questionable as to whether this is a true reflection of the sensors' capabilities or a function of the initial sensor orientation as a source of error. Therefore, it is essential to understand the impact of the initial sensor orientation on the measurement of both peak angles and through-range angles. If this error can be quantified, clinicians, coaches, and researchers will be better able to understand the sensor's sensitivity in detecting change relative to the error. Moreover, if error can be corrected, then users can be confident that any values produced are correct and that these are immune to issues of attachment orientation.

This study had the following aims:

- Step 1: Systematically explore the effect of initial sensor orientation and the effect of movement velocity on the error of accelerometer-derived angles, including a method for predicting error based on initial orientation and velocity of motion.

- Step 2: Explore the influence of a proposed algorithm designed to correct errors associated with initial sensor orientation.

We hypothesize (a) that increasing initial sensor orientation will result in increased sensor error; (b) that increasing velocity will result in increased sensor error; and (c) that this can be reduced through mathematical correction.

2. Materials and Methods

To create a single degree of freedom, a custom-made jig was constructed to represent a hinge joint. It was constructed from wood with a metallic hinge (Figure 1), where one 'limb' was fixed to an immobile stand. The other limb was free to bend, with 'stops' at angles (40°, 80°, and 120°) as confirmed via a goniometer.

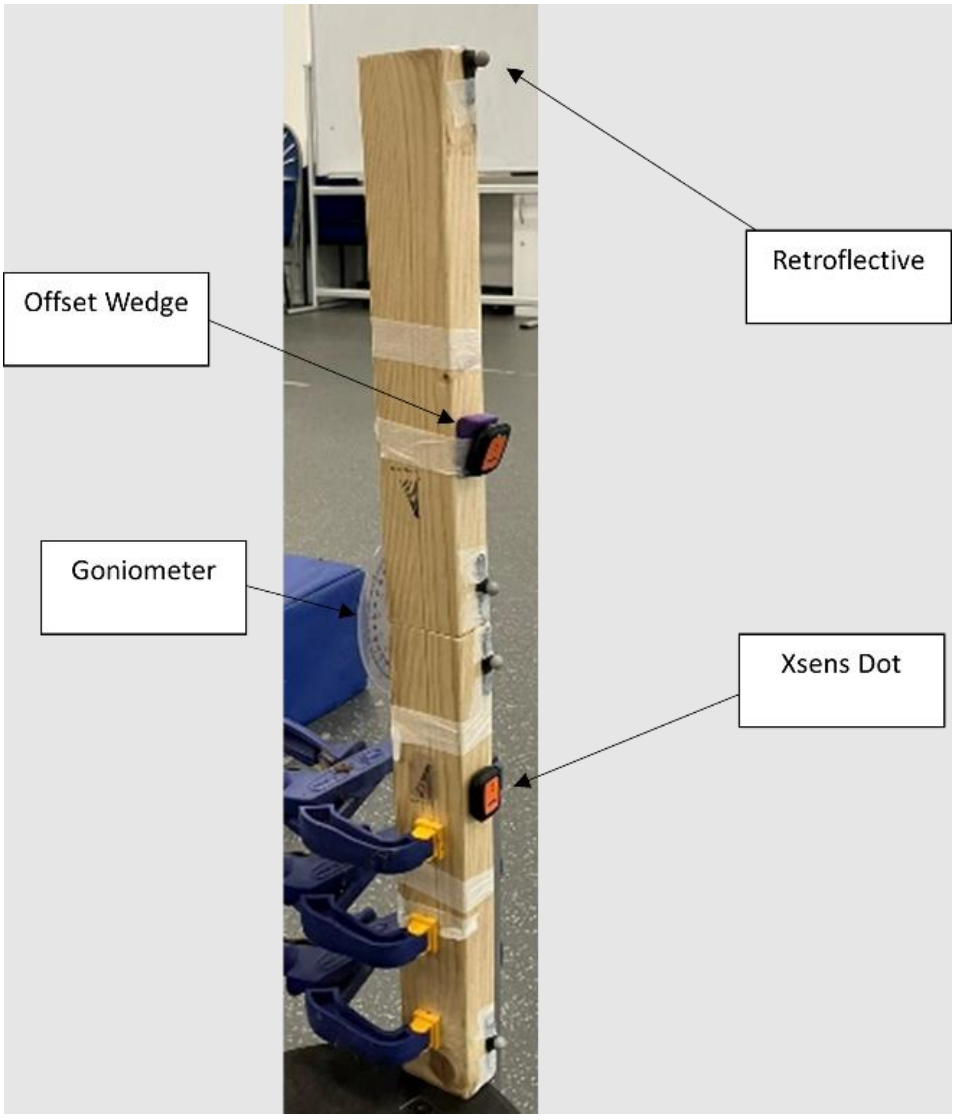

Figure 1. The jig with the IMUs attached to bottom and top section.

Each wooden limb was instrumented with an IMU (Movella Xsens Dots, Enschede, The Netherlands). Such devices house triaxial accelerometers, gyroscopes, and magnetometers and have a reported dynamic orientation accuracy of 1° [26]. This study utilized only the accelerometer for angle derivation operating at 120 Hz. Two retroreflective markers were attached at the top and bottom of each limb to create individual limbs in the motion analysis software to calculate the joint angle using an eight-camera Qualisys Opus 7+ optoelectronic motion (OEM) (Qualisys, Gothenburg, Sweden) capture system, operating

as the reference gold standard recording at 120 Hz. A third IMU (not attached to the jig) with an attached retroreflective marker was used to time-synchronize the accelerometer data with the OEM data.

2.1. Procedure

To explore the influence of initial sensor orientation (sensor offset angle), a systematic approach to increasing, gradually, the initial sensor orientation offset was taken using a series of custom-made wedges to offset the sensor in the non-primary motion planes as described below (Figure 1).

To simulate forward-bending movements (rotation about Y in Figure 2), the initial orientation was gradually increased from 0° to 20° of tilt (rotation about Z in Figure 2), from 0° to 20° of twist (rotation about X in Figure 2), and then via a combination of tilt and twist in 5° increments. These offsets were informed by preliminary testing where the initial sensor orientation offset could reach 20°. To simulate lateral bending movements, the initial sensor orientation was gradually increased through 0° to 50° pitch (rotation about Y in Figure 2) in 10° increments, from 0° to 20° of twist (rotation about X) in 5° increments, and via a combination of pitch and twist. Larger pitch angles were explored due to the reported sacral pitch angles commonly reaching 50° [27].

Figure 2. The Movella Dot inertial measurement unit with sensor axes alignment.

Once the initial orientation was established, the jig was moved through 40°, 80°, and 120° of simulated forward bending, or 40° and 80° of simulated lateral bending, with each movement repeated three times for each bending angle and each sensor orientation.

To explore the effects of movement velocity on the resultant angle measurement, the jig was moved through a range of movement velocities guided by a metronome set at a slow velocity (0.5 Hz) and a fast velocity (1 Hz) to match known movement velocities [12,24,28,29]. This was repeated for the series of increasing tilt and twist offsets described above.

2.2. Data Processing and Analysis

Data processing and analysis used custom-written algorithms in MATLAB (Mathworks, 2021). All data were filtered using a 4th-order low-pass Butterworth filter with a cut-off of 1 Hz. This cut-off frequency was chosen as it provides a balance between smoothing the data and preventing aliasing, with no influence on levels of agreement between OEM and accelerometer-derived angles [10]. Tangents from the OEM data were used to compute the resultant angle between the two 'limbs' of the jig and served as the gold standard reference. Limits of agreement (95%) were calculated between the accelerometer-derived angles and OEM angles. Only accelerometer data were used from the IMU sensors due to the known challenges of metallic environments and gyroscopic drift [15].

Data Analysis and Statistics: Step 1 The effect of initial sensor orientation on the error of accelerometer-derived angles.

To achieve the aim outlined in step 1, angles were derived from the accelerometer using the 4-quadrant arc tangent function (ATAN2), with the absolute sagittal movement of each sensor (flexion extension (rotation about Y)) calculated from acceleration X and Z, and the absolute frontal movement from each sensor (lateral bending (rotation about Z)) calculated from acceleration X and Y. The resultant angle was calculated through angle subtraction between the two absolute sensor angles.

The effect of the initial orientation on the error of the angle computation was explored through direct comparison to simultaneously captured OEM data. Peak range of motion (ROM) estimates (40°, 80°, and 120° forward bending and 40° and 80° lateral bending) were compared, with root mean square errors (RMSE) and 95% confidence intervals (CI95%) being calculated.

Error estimates for different initial orientations were plotted and fitted with a linear regression function to provide estimates of error based on the initial orientation. Data were also explored for reliability though intraclass correlation coefficients (ICC $_{2,1}$) for peak ROM.

Accelerometer-derived angles and OEM angles were analyzed through the whole ROM to explore the effect of movement velocity on the RMSE between the data. OEM data were differentiated to yield angular velocity, and data where movement was 'static' (<1° s^{-1}) were removed from the analysis. Therefore, RMSE for angles between the accelerometer and OEM were established across a range of velocities up to 148° s^{-1}, and velocities were sub-classified into slow (average 49° s^{-1} ± 11° s^{-1}) and fast (average 83° s^{-1} ± 24° s^{-1}) to facilitate predictive equation fitting.

3. Results

3.1. Results for Step 1

The angles produced from the accelerometer demonstrated excellent reliability with ICC values for repeated trials above 0.95 for both forward and lateral bending. This demonstrates that reliability is not a function of initial sensor orientation.

Error analysis for accelerometer-derived angles compared to OEM in the forward-bending plane (rotation about Y) across different initial orientation offsets is presented in Figure 3A–C. It demonstrates that error increases as the initial orientation offset increases, with limits of agreement ranging from −1.65° to 4.38°. The most extreme offset measured (20° tilt (rotation about Z) and 20° twist (rotation about X)) produced an average RMSE of 5.86°.

In the lateral-bending plane (rotation about Z), the error for different initial orientation offsets is presented in Figure 4A–C. These demonstrate that error increases as the initial orientation offset increases, with limits of agreement ranging from –2.82° to 6.18°. The most extreme offset measured (50° pitch (rotation about Y) and 20° twist (rotation about X)) resulted in an average RMSE of 7.54°.

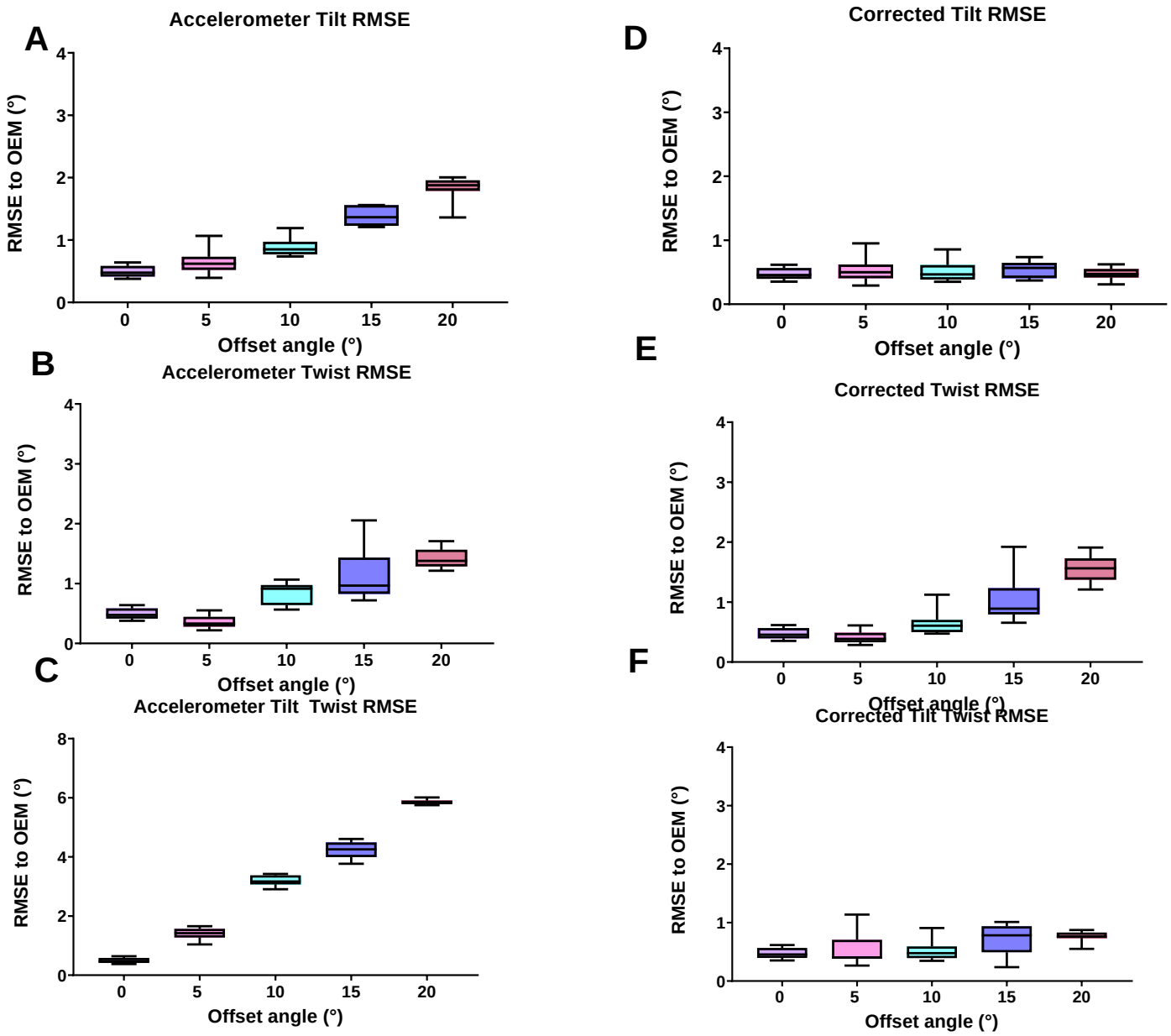

Figure 3. Root mean square error (RMSE) box plots of sagittal plane bending. (**A**) Accelerometer RMSE compared to motion capture for increasing tilt offsets. (**B**) Accelerometer RMSE compared to motion capture for increasing twist offsets. (**C**) Accelerometer RMSE compared to motion capture for tilt and twist offsets together. (**D**) Corrected-method RMSE compared to motion capture for increasing tilt offsets. (**E**) Corrected-method RMSE compared to motion capture for increasing twist offsets. (**F**) Corrected-method RMSE compared to motion capture for tilt and twist offsets together.

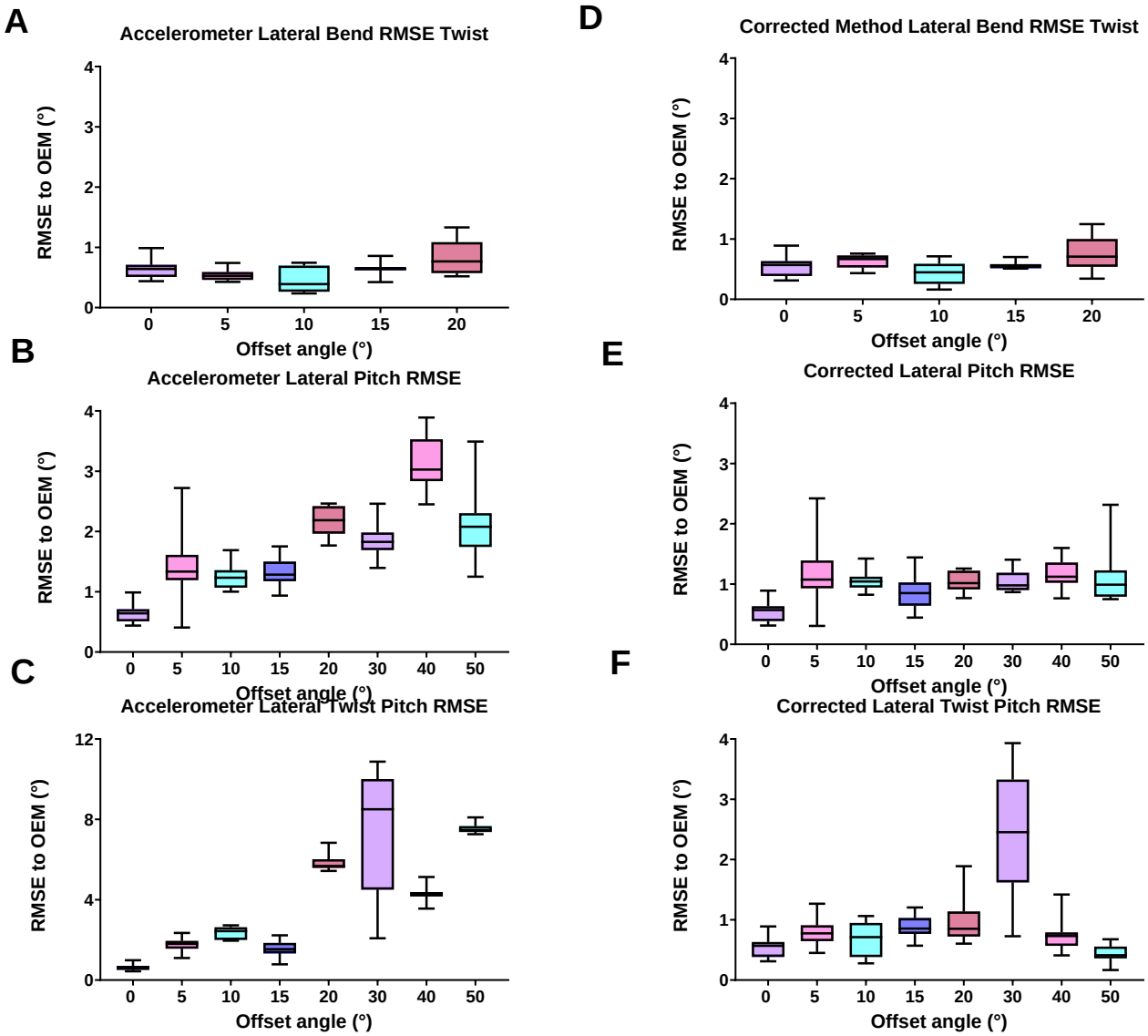

Figure 4. Root mean square error (RMSE) box plots of frontal plane bending. (**A**) Accelerometer RMSE compared to motion capture for increasing twist offsets. (**B**) Accelerometer RMSE compared to motion capture for increasing pitch offsets. (**C**) Accelerometer RMSE compared to motion capture for increasing twist and pitch offset together. (**D**) Corrected-method RMSE compared to motion capture for twist offsets. (**E**) Corrected-method RMSE compared to motion capture for pitch offsets. (**F**) Corrected-method RMSE compared to motion capture for twist and pitch offsets together.

3.2. Equation for Error Prediction—Peak Values

Linear fit equations and R^2 values (goodness of fit) are presented in Table 1 for peak values.

Therefore, for an initial sensor orientation with zero tilt but 18° twist, an expected error of 1.3° can be predicted for movement in the sagittal plane and of 0.8° in the frontal plane. Furthermore, if a sensor is mounted with 25° tilt and 25° twist, a predicted error of 7.1° for movements in the sagittal plane can be expected. Predictive modeling estimated a 3.2° increase in peak sagittal plane error for every 10° increase in tilt and twist, and a 2.3° increase in frontal plane error for every 10° increase in pitch and twist.

Table 1. Linear fit equations for both sagittal and frontal plane movements, for each of the offset variations.

Sagittal Plane Movement	Equation	R^2	Frontal Plane Movement	Equation	R^2
Tilt Offset (rot. about Z)	Y = 0.0695x + 0.3081	0.975	Pitch offset (rot. about Y)	Y = 0.0250x + 1.1057	0.464
Twist Offset (rot. about X)	Y = 0.0558x + 0.2592	0.816	Twist offset (rot. about X)	Y = 0.0127x + 0.5408	0.362
Tilt/Twist Dual Offset	Y = 0.2514x + 0.7703	0.960	Pitch/Twist offset	Y = 0.1115x + 1.1739	0.741

Notes. Rot.: rotation; X: initial orientation angle; Y: error prediction in degrees.

3.3. Through-Range Analysis

Through-range analysis demonstrated that the jig was moved across velocities ranging from 1° s^{-1} to 148° s^{-1}, where the typical lumbar flexion/extension movement velocity is reported as 25–43° s^{-1} and ~17–55° s^{-1} ([28], estimated from Figure 3 [30]). Offset was plotted against RMSE for slow (average 49° s^{-1} ± 11° s^{-1}) and fast (average 83° s^{-1} ± 24° s^{-1}) velocity, demonstrating little difference in the error for the two velocities. Data were fit with a linear regression (R^2 = 0.988; y = 0.3725x + 0.7654 for slow, and R^2 = 0.987; y = 0.3189x + 0.5656 for fast), demonstrating a strong relationship between offset angle and RMSE during the movement phase (Figure 5).

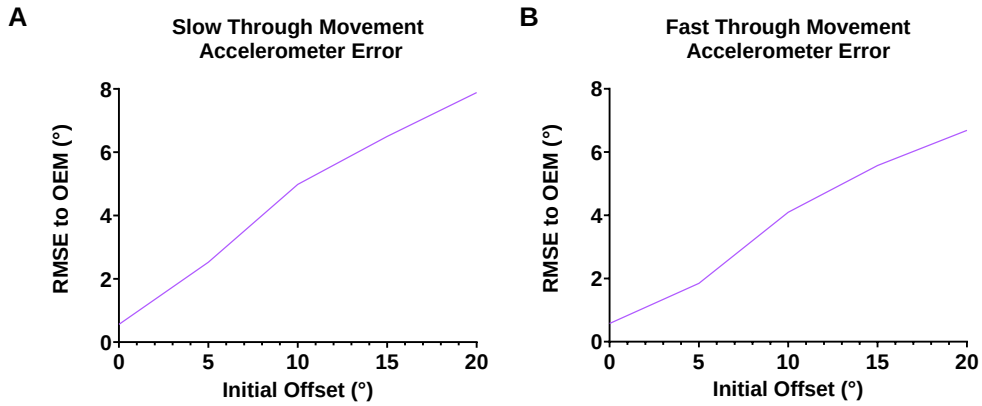

Figure 5. Average through movement RMSE for each time point where angular velocity is greater than 1° s^{-1} across dual offsets of tilt and twist. (**A**) Slow movement trials: 0.5 Hz average 49° s^{-1} ± 11° s^{-1}. (**B**) Fast movement trials: 1 Hz average 83° s^{-1} ± 24° s^{-1}.

Therefore, for a sensor mounted with 25° of tilt and twist, moving at an angular velocity of around 49° s^{-1}, an error of 10.1° can be expected, demonstrating slightly greater predicted error during movement compared to a static predicted error of 7.1°. Predictive modeling estimated a 3.7° increase in through-range sagittal plane error for every 10° increase in tilt and twist initial sensor orientation offset.

To explore the overall effect of velocity on error across all the offsets, velocity was plotted against RMSE (Figure 6), with the mean RMSE values being presented in Table 2.

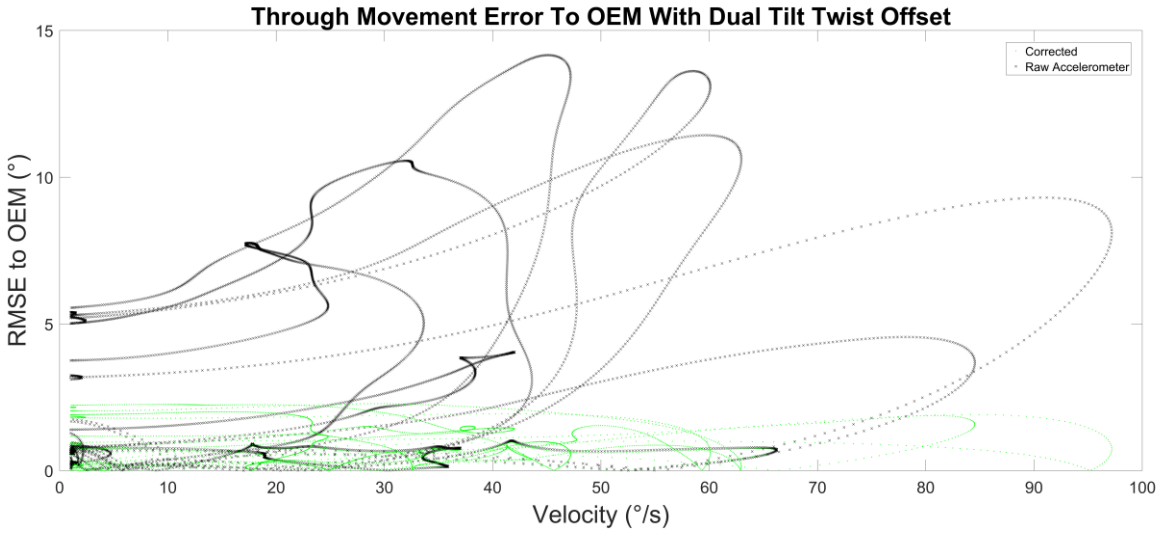

Figure 6. Through-movement RMSE against speed for every data point where the angular velocity is greater than 1° s^{-1}, showing the differences in relationship between error and speed for the accelerometer data and the corrected data. RMSE—Root mean square error.

Table 2. Average through-movement RMSE from each data point where angular velocity is greater than 1° s^{-1}.

		Initial Offset Tilt and Twist (°)				
		0	**5**	**10**	**15**	**20**
Initial Offset Tilt and Twist (°)	Accelerometer Slow RMSE (°)	0.56	2.52	4.98	6.50	7.89
	Accelerometer Fast RMSE (°)	0.58	1.85	4.09	5.57	6.69
	Corrected Slow RMSE (°)	0.53	1.19	0.51	1.05	1.19
	Corrected Fast RMSE (°)	0.53	0.67	0.98	1.19	1.18

Notes: RMSE: Root mean square error; Slow: 0.5 Hz average 49° s^{-1} ± 11° s^{-1}; Fast: 1 Hz average 83° s^{-1} ± 24° s^{-1}.

3.4. Data Analysis and Statistics: Step 2 The Effect of Initial Sensor Orientation Angle Correction

To achieve the aim outlined in step 2, the same data were used to explore the influence of a mathematical correction algorithm. The initial orientation of the sensor was calculated using the algorithm above (ATAN2), from which an orientation quaternion (Qi) was computed. Corrected acceleration data were generated through the rotation of the existing data via the following input:

$$\text{Corrected Accelerometer Data} = -\text{Qi} \times \text{Accelerometer data},$$

where Qi is the quaternion representation of the initial orientation. From these corrected acceleration data, forward bending and lateral bending were computed using the ATAN2 function as before.

The effect of the correction on the error of the angle computation was explored using identical approaches outlined in step 1 above. Briefly, for peak ROM, estimates compared to OEM, RMSE, and 95% confidence intervals (CI95%) were calculated. The reliability of peak estimates as explored though intraclass correlation coefficients ($ICC_{2,1}$). Through-range analysis for the non-static portions of the curve was used to compute RMSE between the OEM and the corrected accelerometer angles across a range of velocities up to 148° s^{-1}, and velocities were sub-classified into slow (average 49° s^{-1} ± 11° s^{-1}) and fast (average 83° s^{-1} ± 24° s^{-1}).

3.5. Results for Step 2

Having applied the correction algorithm, the peak values produced from the corrected accelerometer were highly reliable, with ICC values for repeat trials being above 0.95 for both forward and lateral bending.

Error analysis for the corrected accelerometer angles compared to OEM in the forward-bending plane (rotation about Y) across different initial orientation offsets is presented in Figure 3D–F. Limits of agreement ranged from −0.49° to 1.52°. The most extreme offset measured (20° tilt (rotate about Z) and 20° twist (rotate about X)) resulted in an average RMSE of 0.75° (uncorrected RMSE of 5.86°).

In the lateral-bending plane (rotation about Z), the error for the corrected accelerometer across different initial orientation offsets is presented in Figure 4D–F. Limits of agreement ranged from −0.47° to 1.68°. At the most extreme offset (50° pitch (rotation about Y) and 20° twist (rotation about X)), the average RMSE was 0.79° (uncorrected RMSE of 7.54°).

Through-range analysis for corrected accelerometer angles demonstrated that with increasing tilt and twist offset and increasing velocity, error remains consistently below 2.3° (Figure 6). Average RMSE for the through-movement portions of the graph across offsets for slow (average 49° s^{-1} ± 11° s^{-1}) and fast (average 83° s^{-1} ± 24° s^{-1}) velocity are presented in Table 2 and are consistently below 1.2°.

4. Discussion

This study set out to systematically evaluate the effect of the initial sensor orientation on the error from accelerometer-derived angles against optoelectronic motion-capture-derived angles (step 1). A mathematical method of correction to reduce these errors was then proposed (step 2).

Results (step 1) demonstrated that using accelerometer data to derive angles results in increasing errors proportional to the initial orientation angle from the optimum, and this feature is accentuated during dynamic (versus static) movement.

Previously studies calculating peak ROM angles, in comparison to a gold standard, have reported limits of agreement ranging from –8.06° to 5.67° [25] and −3.86° to 4.69° [11]. Data from the current study showed similar but tighter limits of agreement (−1.65° to 4.38°) prior to correction, and therefore it is possible that some of the range of these errors is due to sensor orientation, especially as no mention of orientation correction was made in these works. Furthermore, previous studies have reported changes in accelerometer-derived pelvis ROM in idiopathic scoliosis [31] and knee ROM errors [32] of 4.5° and 2.4°, respectively [31,32]. As demonstrated in step 1, it is also possible that this magnitude of error relates to attachment orientation, especially with the known obliquity of the spine with scoliosis [33].

The current study extends the analysis from peak ROM errors to through-range errors, contributing to the evidence of using the sensors in an ecologically valid manner. This required the exploration of the effect of movement velocity on sensor error. Previous studies have explored angular velocity through differentiation of accelerometer-derived angles, but it is not clear if any correction for orientation was completed [20]. However, no studies have systematically explored the relationship between error and velocity or the effect of a mathematical correction.

The current findings suggest that without correction for orientation, the RMSE through-movement is a function of velocity (Figure 6), illustrated through dynamic errors being larger than static errors. This is the first study to explore this for accelerometer-derived angles. Uncorrected error values were similar to previous studies that have reported dynamic errors of around 7° for accelerometers moving through a single plane of motion [34]. These findings imply that utilizing 'off-the-shelf accelerometers' for motion analysis warrants caution, particularly when uncorrected data are employed.

A significant contribution from this work is the production of error prediction equations, enabling users to determine the likely error expected from accelerometer-derived angles. This can serve as a useful tool for planning data collection or correcting existing

data, where the expected magnitude of change from an intervention, for example, can be compared to the magnitude of error. Interestingly, the error associated with orientation offset in two axes is cumulative such that it is of greater magnitude than that of the tilt error plus the twist error (Figure 3A–C) and is compounded during dynamic movement. The linear regression 'goodness of fit' was excellent for the sagittal plane regardless of velocity, but lower for the frontal plane. Therefore, caution is advised when using it to estimate error as the prediction is less likely to represent the value authentically. However, the R^2 for dual offsets (>0.74) suggest that a good prediction of error in the frontal plane is still possible, and when applied to the real-world testing of individuals, sensor attachment is likely to feature offsets in both planes.

Reliability was shown to be excellent regardless of initial orientation, suggesting that accelerometer-derived angles without correction can be used for repeated measures. However, this would only be the case if the sensors were not removed so as to avoid introducing reattachment orientation error. Lower estimates of between-day reliability commonly feature in the literature [8,35], where some of the additional error may be due to initial sensor orientation. The mathematical correction demonstrated here suggests that this error can be resolved, removing the variability and effect of differing sensor orientations. The magnitude of resulting errors are within those expected from data specification sheets and match those of other motion analysis methods [36–40]. Using normative ROM data from Van Herp et al. [41], example error for lumbar flexion was reduced by our algorithm from 10.6% in the sagittal plane to 1.4% following correction for a 20° tilt and twist initial orientation. The results of this study also showed no differences in error due to ROM size as limits of agreement across all conditions were below 1.7°. Furthermore, the mathematical correction results in the removal of the relationship between error and velocity, suggesting that accelerometers can be used with confidence within the parameters tested in this study.

Accelerometers have some inherent advantages over other methods. They operate without concern for metallic interference and do not suffer from integration drift; therefore, they are ideal for a breadth of environments and operate well across time. Therefore, accelerometers can offer an attractive option for motion analysis with excellent reliability and small errors, allowing for confidence of use in any environment to measure joint angles.

The knowledge gained from this study allows for confidence in the use of accelerometers for a range of joint angle measurements if the initial orientation is corrected. Initial sensor orientation error goes some way towards explaining the errors between different operators (inter-operator error) and the error associated with removing and reattaching measurement devices (i.e., pre–post attachment orientation error). Therefore, the removal of this source of error means that accelerometers can be used to quantify changes in ROM from interventions (i.e., physiotherapy or surgery) or across time (i.e., with progressive conditions) in a range of locations and environments.

Limitations

It is acknowledged that this study used a jig rather than human testing to remove human variability associated with repeated movement. ROM was tested up to 120° and 148° s^{-1}; results beyond this are not known. Velocity consistency and movement smoothness whilst moving the jig was poorly controlled; however, due to simultaneous data capture, both systems were affected equally.

5. Conclusions

This study systematically demonstrated that accelerometer-derived angles are subject to error based on uncorrected initial offset, and that the magnitude of error has a linear relationship with the initial orientation. The magnitude of error was greater during dynamic movement and was greater when two non-primary plane offsets were present. Furthermore, it was determined that these errors were reduced through the correction algorithm proposed. Therefore, having established validity (following the application of the correction algorithm) and reliability, accelerometers can be used for motion analysis.

Future studies should look at real-world applications of these sensors to quantify human movement or performance without the problems of orientation-induced error.

Author Contributions: Conceptualization, F.A.M., A.J.C. and J.M.W.; methodology, F.A.M., A.J.C. and J.M.W.; writing—original draft preparation, F.A.M.; writing—review and editing, A.J.C., C.J.C. and J.M.W.; supervision, A.J.C., C.J.C. and J.M.W.; All authors have read and agreed to the published version of the manuscript.

Funding: This research received no external funding.

Institutional Review Board Statement: Not applicable.

Informed Consent Statement: Not applicable.

Data Availability Statement: Data available through http://bordar.bournemouth.ac.uk/342/ (accessed on 15 January 2023).

Conflicts of Interest: The authors declare no conflicts of interest.

References

1. Cuesta-Vargas, A.I.; Galán-Mercant, A.; Williams, J.M. The use of inertial sensors system for human motion analysis. *Phys. Ther. Rev.* **2010**, *15*, 462–473. [CrossRef]
2. Matthew, R.P.; Seko, S.; Bajcsy, R.; Lotz, J. Kinematic and kinetic validation of an improved depth camera motion assessment system using rigid bodies. *IEEE J. Biomed. Heal. Inform.* **2018**, *23*, 1784–1793. [CrossRef]
3. Alqhtani, R.S.; Jones, M.D.; Theobald, P.S.; Williams, J.M. Correlation of Lumbar-Hip Kinematics between Trunk Flexion and Other Functional Tasks. *J. Manip. Physiol. Ther.* **2015**, *38*, 442–447. [CrossRef]
4. Lee, R.Y.; Laprade, J.; Fung, E.H. A real-time gyroscopic system for three-dimensional measurement of lumbar spine motion. *Med. Eng. Phys.* **2003**, *25*, 817–824. [CrossRef]
5. Williams, J.M.; Haq, I.; Lee, R.Y. An experimental study investigating the effect of pain relief from oral analgesia on lumbar range of motion, velocity, acceleration and movement irregularity. *BMC Musculoskelet. Disord.* **2014**, *15*, 304. [CrossRef]
6. Alqhtani, R.S.; Jones, M.D.; Theobald, P.S.; Williams, J.M. Reliability of an accelerometer-based system for quantifying multiregional spinal range of motion. *J. Manip. Physiol. Ther.* **2015**, *38*, 275–281. [CrossRef]
7. Bauer, C.M.; Rast, F.M.; Ernst, M.J.; Kool, J.; Oetiker, S.; Rissanen, S.M.; Suni, J.H.; Kankaanpää, M. Concurrent validity and reliability of a novel wireless inertial measurement system to assess trunk movement. *J. Electromyogr. Kinesiol.* **2015**, *25*, 782–790. [CrossRef] [PubMed]
8. Williams, J.M.; Haq, I.; Lee, R.Y. A novel approach to the clinical evaluation of differential kinematics of the lumbar spine. *Man. Ther.* **2013**, *18*, 130–135. [CrossRef]
9. Senington, B.; Lee, R.Y.; Williams, J.M. Validity and reliability of innovative field measurements of tibial accelerations and spinal kinematics during cricket fast bowling. *Med. Biol. Eng. Comput.* **2021**, *59*, 1475–1484. [CrossRef]
10. Williams, J.M.; Frey, M.; Breen, A.; De Carvalho, D. Systematic analysis of different low-pass filter cut-off frequencies on lumbar spine kinematics data and the impact on the agreement between accelerometers and an optoelectronic system. *J. Biomech.* **2022**, *145*, 111395. [CrossRef]
11. Mjøsund, H.L.; Boyle, E.; Kjaer, P.; Mieritz, R.M.; Skallgård, T.; Kent, P. Clinically acceptable agreement between the ViMove wireless motion sensor system and the Vicon motion capture system when measuring lumbar region inclination motion in the sagittal and coronal planes. *BMC Musculoskelet. Disord.* **2017**, *18*, 124. [CrossRef]
12. Beange, K.H.; Chan, A.D.; Beaudette, S.M.; Graham, R.B. Concurrent validity of a wearable IMU for objective assessments of functional movement quality and control of the lumbar spine. *J. Biomech.* **2019**, *97*, 109356. [CrossRef]
13. Piche, E.; Guilbot, M.; Chorin, F.; Guerin, O.; Zory, R.; Gerus, P. Validity and repeatability of a new inertial measurement unit system for gait analysis on kinematic parameters: Comparison with an optoelectronic system. *Measurement* **2022**, *198*, 111442. [CrossRef]
14. Franco, L.; Sengupta, R.; Wade, L.; Cazzola, D. A novel IMU-based clinical assessment protocol for Axial Spondyloarthritis: A protocol validation study. *PeerJ* **2021**, *9*, e10623. [CrossRef] [PubMed]
15. Weygers, I.; Kok, M.; De Vroey, H.; Verbeerst, T.; Versteyhe, M.; Hallez, H.; Claeys, K. Drift-free inertial sensor-based joint kinematics for long-term arbitrary movements. *IEEE Sens. J.* **2020**, *20*, 7969–7979. [CrossRef]
16. Madgwick, S.O.H.; Wilson, S.; Turk, R.; Burridge, J.; Kapatos, C.; Vaidyanathan, R. An extended complementary filter for full-body marg orientation estimation. *IEEE/ASME Trans. Mechatron.* **2020**, *25*, 2054–2064. [CrossRef]
17. de Vries, W.; Veeger, H.; Baten, C.; van der Helm, F. Magnetic distortion in motion labs, implications for validating inertial magnetic sensors. *Gait Posture* **2009**, *29*, 535–541. [CrossRef]
18. Fisher, C.J. *Using an Accelerometer for Inclination Sensing*; AN-1057, Application Note; Analog Devices: Norwood, MA, USA, 2010; pp. 1–8.

19. Luinge, H.J.; Veltink, P.H. Measuring orientation of human body segments using miniature gyroscopes and accelerometers. *Med. Biol. Eng. Comput.* **2005**, *43*, 273–282. [CrossRef]
20. Alqhtani, R.S.; Jones, M.D.; Theobald, P.S.; Williams, J.M. Investigating the contribution of the upper and lower lumbar spine, relative to hip motion, in everyday tasks. *Man. Ther.* **2016**, *21*, 268–273. [CrossRef]
21. Fiorentino, N.M.; Atkins, P.R.; Kutschke, M.J.; Goebel, J.M.; Foreman, K.B.; Anderson, A.E. Soft tissue artifact causes significant errors in the calculation of joint angles and range of motion at the hip. *Gait Posture* **2017**, *55*, 184–190. [CrossRef] [PubMed]
22. Xi, X.; Ling, Z.; Wang, C.; Gu, C.; Zhan, X.; Yu, H.; Lu, S.; Tsai, T.-Y.; Yu, Y.; Cheng, L. Lumbar segment-dependent soft tissue artifacts of skin markers during in vivo weight-bearing forward–Backward bending. *Front. Bioeng. Biotechnol.* **2022**, *10*, 960063. [CrossRef]
23. Dunk, N.M.; Callaghan, J.P. Lumbar spine movement patterns during prolonged sitting differentiate low back pain developers from matched asymptomatic controls. *Work* **2010**, *35*, 3–14. [CrossRef]
24. Ma, J.; Kharboutly, H.; Benali, A.; Benamar, F.; Bouzit, M. Joint angle estimation with accelerometers for dynamic postural analysis. *J. Biomech.* **2015**, *48*, 3616–3624. [CrossRef]
25. Chang, R.P.; Smith, A.; Kent, P.; Saraceni, N.; Hancock, M.; O'sullivan, P.B.; Campbell, A. Concurrent validity of DorsaVi wireless motion sensor system Version 6 and the Vicon motion analysis system during lifting. *BMC Musculoskelet. Disord.* **2022**, *23*, 909. [CrossRef]
26. Movella Xsens Dots. Products | Movella.com. 2023. Available online: https://movella.com/products/wearables/movella-dot (accessed on 2 December 2023).
27. Legaye, J. The femoro-sacral posterior angle: An anatomical sagittal pelvic parameter usable with dome-shaped sacrum. *Eur. Spine J.* **2007**, *16*, 219–225. [CrossRef]
28. Consmüller, T.; Rohlmann, A.; Weinland, D.; Druschel, C.; Duda, G.N.; Taylor, W.R. Velocity of lordosis angle during spinal flexion and extension. *PLoS ONE* **2012**, *7*, e50135. [CrossRef] [PubMed]
29. Chen, H.; Schall, M.C., Jr.; Fethke, N. Effects of movement speed and magnetic disturbance on the accuracy of inertial measurement units. In Proceedings of the Human Factors and Ergonomics Society Annual Meeting, Austin, TX, USA, 9–13 October 2017; SAGE Publications: Los Angeles, CA, USA, 2017; Volume 61, pp. 1046–1050.
30. Shum, G.L.K.; Crosbie, J.; Lee, R.Y.W. Effect of low back pain on the kinematics and joint coordination of the lumbar spine and hip during sit-to-stand and stand-to-sit. *Spine* **2005**, *30*, 1998–2004. [CrossRef] [PubMed]
31. Jamison, M.; Glover, M.; Peterson, K.; DeGregorio, M.; King, K.; Danelson, K.; O'gara, T. Lumbopelvic postural differences in adolescent idiopathic scoliosis: A pilot study. *Gait Posture* **2022**, *93*, 73–77. [CrossRef]
32. McGinnis, R.S.; Patel, S.; Silva, I.; Mahadevan, N.; DiCristofaro, S.; Jortberg, E.; Ceruolo, M.; Aranyosi, A.J. Skin mounted accelerometer system for measuring knee range of motion. In Proceedings of the 2016 38th Annual International Conference of the IEEE Engineering in Medicine and Biology Society (EMBC), Orlando, FL, USA, 16–20 August 2016; pp. 5298–5302.
33. Jimbo, S.; Kobayashi, T.; Aono, K.; Atsuta, Y.; Matsuno, T. Epidemiology of degenerative lumbar scoliosis: A community-based cohort study. *Spine* **2012**, *37*, 1763–1770. [PubMed]
34. Bittel, A.J.; Elazzazi, A.; Bittel, D.C. Accuracy and precision of an accelerometer-based smartphone app designed to monitor and record angular movement over time. *Telemed. e-Health* **2016**, *22*, 302–309. [CrossRef]
35. Miyachi, R.; Sano, A.; Tanaka, N.; Tamai, M.; Miyazaki, J. Measuring Lumbar Motion Angle with a Small Accelerometer: A Reliability Study. *J. Chiropr. Med.* **2022**, *21*, 32–38. [CrossRef] [PubMed]
36. Hagemeister, N.; Parent, G.; Husse, S.; de Guise, J.A. A simple and rapid method for electromagnetic field distortion correction when using two Fastrak sensors for biomechanical studies. *J. Biomech.* **2008**, *41*, 1813–1817. [CrossRef] [PubMed]
37. Williams, J.M.; Haq, I.; Lee, R.Y. Dynamic measurement of lumbar curvature using fibre-optic sensors. *Med. Eng. Phys.* **2010**, *32*, 1043–1049. [CrossRef] [PubMed]
38. Robert-Lachaine, X.; Mecheri, H.; Larue, C.; Plamondon, A. Validation of inertial measurement units with an optoelectronic system for whole-body motion analysis. *Med. Biol. Eng. Comput.* **2017**, *55*, 609–619. [CrossRef] [PubMed]
39. Robert-Lachaine, X.; Mecheri, H.; Muller, A.; Larue, C.; Plamondon, A. Validation of a low-cost inertial motion capture system for whole-body motion analysis. *J. Biomech.* **2020**, *99*, 109520. [CrossRef]
40. Burkhart, K.; Grindle, D.; Bouxsein, M.L.; Anderson, D.E. Between-session reliability of subject-specific musculoskeletal models of the spine derived from optoelectronic motion capture data. *J. Biomech.* **2020**, *112*, 110044. [CrossRef]
41. Van Herp, G.; Rowe, P.; Salter, P.; Paul, J.P. Three-dimensional lumbar spine kinematics: A study of range of movement in 100 healthy subjects aged 20 to 60+ years. *Rheumatology* **2000**, *39*, 1337–1340.